ISSN 1007-9327 (print)
ISSN 2219-2840 (online)

World Journal of *Gastroenterology*

World J Gastroenterol 2022 June 21; 28(23): 2527-2635

Published by Baishideng Publishing Group Inc

World Journal of Gastroenterology

Contents

Weekly Volume 28 Number 23 June 21, 2022

REVIEW

2527 Autoimmune liver diseases in systemic rheumatic diseases

Wang CR, Tsai HW

2546 Fecal microbiota transplantation in the metabolic diseases: Current status and perspectives

Zheng L, Ji YY, Wen XL, Duan SL

MINIREVIEWS

2561 Up to seven criteria in selection of systemic therapy for hepatocellular carcinoma

Silk T, Silk M, Wu J

ORIGINAL ARTICLE

Basic Study

2569 Family with sequence similarity 134 member B-mediated reticulophagy ameliorates hepatocyte apoptosis induced by dithiothreitol

Guo YX, Han B, Yang T, Chen YS, Yang Y, Li JY, Yang Q, Xie RJ

Retrospective Study

2582 Infliximab trough level combined with inflammatory biomarkers predict long-term endoscopic outcomes in Crohn's disease under infliximab therapy

Cao WT, Huang R, Liu S, Fan YH, Xu MS, Xu Y, Ni H

2597 Higher infliximab and adalimumab trough levels are associated with fistula healing in patients with fistulising perianal Crohn's disease

Gu B, Venkatesh K, Williams AJ, Ng W, Corte C, Gholamrezaei A, Ghaly S, Xuan W, Paramsothy S, Connor S

2609 Whole lesion histogram analysis of apparent diffusion coefficient predicts therapy response in locally advanced rectal cancer

Jiménez de los Santos ME, Reyes-Pérez JA, Domínguez Osorio V, Villaseñor-Navarro Y, Moreno-Astudillo L, Vela-Sarmiento I, Sollozo-Dupont I

CASE REPORT

2625 Primary gastric dedifferentiated liposarcoma resected endoscopically: A case report

Cho JH, Byeon JH, Lee SH

LETTER TO THE EDITOR

2633 Reconstructing the puzzle of the role of therapeutic endoscopy in the management of post-bariatric surgery complications

Argyriou K, Parra-Blanco A

ABOUT COVER

Editorial Board Member of *World Journal of Gastroenterology*, Osamu Toyoshima, MD, Director, Department of Gastroenterology, Toyoshima Endoscopy Clinic, 6-17-5 Seijo, Setagaya-ku, Tokyo 157-0066, Japan. t@ichou.com

AIMS AND SCOPE

The primary aim of *World Journal of Gastroenterology* (*WJG*, *World J Gastroenterol*) is to provide scholars and readers from various fields of gastroenterology and hepatology with a platform to publish high-quality basic and clinical research articles and communicate their research findings online. *WJG* mainly publishes articles reporting research results and findings obtained in the field of gastroenterology and hepatology and covering a wide range of topics including gastroenterology, hepatology, gastrointestinal endoscopy, gastrointestinal surgery, gastrointestinal oncology, and pediatric gastroenterology.

INDEXING/ABSTRACTING

The *WJG* is now indexed in Current Contents®/Clinical Medicine, Science Citation Index Expanded (also known as SciSearch®), Journal Citation Reports®, Index Medicus, MEDLINE, PubMed, PubMed Central, and Scopus. The 2021 edition of Journal Citation Report® cites the 2020 impact factor (IF) for *WJG* as 5.742; Journal Citation Indicator: 0.79; IF without journal self cites: 5.590; 5-year IF: 5.044; Ranking: 28 among 92 journals in gastroenterology and hepatology; and Quartile category: Q2. The *WJG*'s CiteScore for 2020 is 6.9 and Scopus CiteScore rank 2020: Gastroenterology is 19/136.

RESPONSIBLE EDITORS FOR THIS ISSUE

NAME OF JOURNAL
World Journal of Gastroenterology

ISSN
ISSN 1007-9327 (print) ISSN 2219-2840 (online)

LAUNCH DATE
October 1, 1995

FREQUENCY
Weekly

EDITORS-IN-CHIEF
Andrzej S Tarnawski

EDITORIAL BOARD MEMBERS
http://www.wjgnet.com/1007-9327/editorialboard.htm

PUBLICATION DATE
June 21, 2022

INSTRUCTIONS TO AUTHORS
https://www.wjgnet.com/bpg/gerinfo/204

GUIDELINES FOR ETHICS DOCUMENTS
https://www.wjgnet.com/bpg/GerInfo/287

GUIDELINES FOR NON-NATIVE SPEAKERS OF ENGLISH
https://www.wjgnet.com/bpg/gerinfo/240

PUBLICATION ETHICS
https://www.wjgnet.com/bpg/GerInfo/288

PUBLICATION MISCONDUCT
https://www.wjgnet.com/bpg/gerinfo/208

ARTICLE PROCESSING CHARGE
https://www.wjgnet.com/bpg/gerinfo/242

STEPS FOR SUBMITTING MANUSCRIPTS
https://www.wjgnet.com/bpg/GerInfo/239

ONLINE SUBMISSION
https://www.f6publishing.com

World Journal of Gastroenterology

Submit a Manuscript: https://www.f6publishing.com

World J Gastroenterol 2022 June 21; 28(23): 2609-2624

DOI: 10.3748/wjg.v28.i23.2609

ISSN 1007-9327 (print) ISSN 2219-2840 (online)

ORIGINAL ARTICLE

Retrospective Study

Whole lesion histogram analysis of apparent diffusion coefficient predicts therapy response in locally advanced rectal cancer

Mayra Evelia Jiménez de los Santos, Juan Armando Reyes-Pérez, Victor Domínguez Osorio, Yolanda Villaseñor-Navarro, Liliana Moreno-Astudillo, Itzel Vela-Sarmiento, Isabel Sollozo-Dupont

Specialty type: Oncology

Provenance and peer review: Unsolicited article; Externally peer reviewed.

Peer-review model: Single blind

Peer-review report's scientific quality classification

Grade A (Excellent): 0
Grade B (Very good): B
Grade C (Good): C, C
Grade D (Fair): 0
Grade E (Poor): 0

P-Reviewer: Karavaş E, Turkey; Setiawati R, Indonesia; Zhao J, China

Received: September 23, 2021
Peer-review started: September 23, 2021
First decision: November 16, 2021
Revised: November 25, 2021
Accepted: April 22, 2022
Article in press: April 22, 2022
Published online: June 21, 2022

Mayra Evelia Jiménez de los Santos, Juan Armando Reyes-Pérez, Victor Domínguez Osorio, Yolanda Villaseñor-Navarro, Liliana Moreno-Astudillo, Isabel Sollozo-Dupont, Department of Radiology, National Cancer Institute, Mexico 14080, Mexico

Itzel Vela-Sarmiento, Department of Gastrointestinal Surgery, National Cancer Institute, Mexico 14080, Mexico

Corresponding author: Isabel Sollozo-Dupont, PhD, Academic Research, Statistician, Department of Radiology, National Cancer Institute, Av. San Fernando No. 22, Col. Sección XVI Delegación Tlalpan, Mexico 14080, Mexico. sodi8507@gmail.com

Abstract

BACKGROUND

Whole-tumor apparent diffusion coefficient (ADC) histogram analysis is relevant to predicting the neoadjuvant chemoradiation therapy (nCRT) response in patients with locally advanced rectal cancer (LARC).

AIM

To evaluate the performance of ADC histogram-derived parameters for predicting the outcomes of patients with LARC.

METHODS

This is a single-center, retrospective study, which included 48 patients with LARC. All patients underwent a pre-treatment magnetic resonance imaging (MRI) scan for primary tumor staging and a second restaging MRI for response evaluation. The sample was distributed as follows: 18 responder patients (R) and 30 non-responders (non-R). Eight parameters derived from the whole-lesion histogram analysis (ADCmean, skewness, kurtosis, and ADC10th, 25th, 50th, 75th, 90th percentiles), as well as the ADCmean from the hot spot region of interest (ROI), were calculated for each patient before and after treatment. Then all data were compared between R and non-R using the Mann-Whitney U test. Two measures of diagnostic accuracy were applied: the receiver operating characteristic curve and the diagnostic odds ratio (DOR). We also reported intra- and interobserver variability by calculating the intraclass correlation coefficient (ICC).

RESULTS

Post-nCRT kurtosis, as well as post-nCRT skewness, were significantly lower in R

than in non-R (both $P < 0.001$, respectively). We also found that, after treatment, R had a larger loss of both kurtosis and skewness than non-R (Δ%kurtosis and Δskewness, $P < 0.001$). Other parameters that demonstrated changes between groups were post-nCRT ADC10th, Δ%ADC10th, Δ%ADCmean, and ROI Δ%ADCmean. However, the best diagnostic performance was achieved by Δ%kurtosis at a threshold of 11.85% (Area under the receiver operating characteristic curve [AUC] = 0.991, DOR = 376), followed by post-nCRT kurtosis = 0.78 × 10^{-3} mm^2/s (AUC = 0.985, DOR = 375.3), Δskewness = 0.16 (AUC = 0.885, DOR = 192.2) and post-nCRT skewness = 1.59 × 10^{-3} mm^2/s (AUC = 0.815, DOR = 168.6). Finally, intraclass correlation coefficient analysis showed excellent intraobserver and interobserver agreement, ensuring the implementation of histogram analysis into routine clinical practice.

CONCLUSION

Whole-tumor ADC histogram parameters, particularly kurtosis and skewness, are relevant biomarkers for predicting the nCRT response in LARC. Both parameters appear to be more reliable than ADCmean from one-slice ROI.

Key Words: Apparent diffusion coefficient; Diffusion-weighted imaging; Histogram analysis; Magnetic resonance imaging; Locally advanced rectal cancer

Core Tip: Whole-tumor apparent diffusion coefficient (ADC) histogram analysis is an emergent imaging analysis in which every voxel is used to obtain a histogram; it thus provides statistical information about tumors. Our study revealed that ADC histogram profiling is a valuable approach that can help differentiate treatment response in locally advanced rectal cancer. When determining tailored treatments that are associated with minimal morbidities, such as the watch and wait method, an accurate treatment response prediction is critical. Given the limitations of this study, more research is needed to establish the clinical utility of our findings.

Citation: Jiménez de los Santos ME, Reyes-Pérez JA, Domínguez Osorio V, Villaseñor-Navarro Y, Moreno-Astudillo L, Vela-Sarmiento I, Sollozo-Dupont I. Whole lesion histogram analysis of apparent diffusion coefficient predicts therapy response in locally advanced rectal cancer. *World J Gastroenterol* 2022; 28(23): 2609-2624
URL: https://www.wjgnet.com/1007-9327/full/v28/i23/2609.htm
DOI: https://dx.doi.org/10.3748/wjg.v28.i23.2609

INTRODUCTION

Neoadjuvant chemoradiation therapy (nCRT) is the gold standard treatment for patients with locally advanced rectal cancer (LARC), followed by surgical resection and adjuvant chemotherapy[1,2]. After nCRT, the ability to achieve tumor reduction or even a pathological complete response (pCR) is observed in approximately 75% of treated patients, whereas the remainder exhibited no treatment response[3,4]. The ability to predict the response to nCRT is important for patients with potentially curable LARC who wish to explore personalized treatment to expand their therapeutic outcomes[5].

Functional magnetic resonance imaging (MRI) techniques, such as diffusion-weighted imaging (DWI), can provide additional physiological information about a tumor's cellular environment, offering great potential to evaluate the therapeutic response to nCRT[5]. This is because the apparent diffusion coefficient (ADC), a quantitative parameter used to assess water diffusion through tissue in DWI, shows an inverse relationship with tissue cellularity[6]. Viable tumor cells restrict the mobility of water, whereas necrotic tumor cells allow the increased diffusion of water molecules[7].

The possibility that ADC may be associated with the nCRT response has been amply investigated in LARC[8-12]; however, significant correlations have not been found in any studies to date[10]. Inconsistencies in previous findings may be due to a lack of standardized imaging and acquisition techniques[5,11], but they may also be due to the fact that the ADC measurements were performed using a manually drawn region of interest (ROI) from a single slice of the ADC map, which holds limited ability to reflect the actual whole-tumor characteristics[13-15].

In the case of whole-lesion histogram analysis of the ADC, a volumetric ROI is positioned on the entire lesion over contiguous slices and a histogram of ADC values reflecting voxel frequency is constructed, leading to the improved evaluation of heterogeneity[16]. Based on this method, first-order heterogeneity parameters can be obtained, which assess the spectrum of ADC values gained from all

voxels within a volume of interest[17]. A growing number of studies have used ADC histogram parameters, as these analyses provide additional information that can aid in the discrimination between benign and malignant regions, or they can help to better characterize the response to treatment in different tumors, such as ovarian, prostate, and breast cancer[18-21]. The application of whole-volume ADC histogram analysis in rectal tumors is increasing in frequency as well, and the role of this parameter in predicting nCRT is promising but limited[22-25].

The purpose of this study was to investigate the imaging response to nCRT using DWI in patients with LARC. We hypothesized that the ADC histogram-derived parameter might better predict treatment responses to nCRT compared with ADC from the hotspot ROI, as histogram parameters can display the heterogeneous features of tumors.

MATERIALS AND METHODS

Patients

The institutional review board approved this retrospective study, and the requirement to obtain informed consent was waived given the study's retrospective nature. The study population was selected from LARC patients at our institution between February 2015 and October 2020. According to Enkhbaatar *et al*[23], we defined the inclusion criteria as follows: (1) Proven histopathology of rectal adenocarcinoma; (2) greater than stage T2 on pre-nCRT MR imaging; with or without regional lymph node metastases and no distant metastases; (3) pre- and post-nCRT rectal MRI imaging with diffusion-weighted (DW) imaging; (4) long-course nCRT; and (5) surgical resection. Mucinous tumors were excluded from this study.

Forty-eight patients were enrolled in the study (34 men and 14 women; age range: 28–84 years). All patients were further divided into two subgroups based on the pathological response of the primary tumor: responders (R) and non-responders (non-R). Only patients with grade 0 according to the TRG-Ryan system were regarded as patients with a complete pathological response (R), while patients with TRG 1-3 were non-R.

MRI protocol

All images were obtained on a 3T MRI system (Discovery MR 750w GEM®; General Electric Healthcare, Milwaukee, WI, United States) using a phased-array body coil. Intravenous antispasmodic agents were not administered, and patients received no bowel preparation before the MRI examination. Our study groups comprised patients who underwent pre-treatment MRI for primary tumor staging, and a second restaging MRI for response evaluation 6 wk after the completion of nCRT. The scanning protocol is listed in Table 1[23]. In brief, we obtained standard T2-weighted (T2W) spin-echo sequences in axial, coronal, and sagittal directions. To improve tumor tissue visualization (including the delineation of the muscular layer), these planes were planned perpendicular to the main axis of the tumor. Moreover, a T1W spin-echo sequence in an axial direction, as well as an axial non-enhanced DWI with b = 1200 s/mm^2, were acquired. ADC maps were automatically generated using the in-line software provided by the vendor during image acquisition. Additionally, axial, sagittal, and coronal fat-suppressed contrast T1W sequences were acquired and used to suppress the signal from adipose tissue. A gadolinium-based contrast agent (Gd-DTPA, Magnevist; Bayer Schering, Berlin, Germany) was used to enhance the quality of MRI. Representative images of our MRI protocol are provided in Figure 1.

Image analysis

Two radiologists (JARP and MEJ, with 10 years and 5 years of experience in gastrointestinal imaging, respectively) reviewed the imaging studies and performed all tumor measurements on the pre- and post-nCRT images. At the initial review, each radiologist was blinded to the other radiologist's opinion. Also, they were blinded to the pathology results to assess interobserver and intraobserver variability. After that, the two radiologists would hold a discussion to arrive at a final decision by consensus. If a disagreement occurred, another radiologist with 25 years of experience (YVN) aided in making the final decision.

DWI analysis was performed with a workstation using the GE Advantage Workstation 4.6 software featuring the READYVIWER application (2006–2010; General Electric, Boston, MA, United States). On the pre-nCRT b1200 diffusion images, the tumor was defined as a focal mass with high signal intensity in comparison with the signal of the normal adjacent rectal wall. More precisely, the delineated ROIs covered the edge of each lesion, and the ROIs were drawn along the inner margin of the rectal walls to avoid intraluminal gas, water, and other contents. Further, necrotic areas, cysts, and vessels related to each lesion at the corresponding slice were also avoided, as identified on T2WI images. In addition, the highest and lowest slices of the DWI images were excluded given their partial volume effects[24]. After nCRT, the tumor was defined by focal areas of residual high signal, as identified on the b1200 images within the location of the primary tumor bed and/or corresponding with the residual tumor on T2WI MRI images as a reference standard. To compare and identify the tumor location, the pre-treatment images were at the readers' disposal when analyzing the post-treatment images.

Table 1 Magnetic resonance imaging sequences and data acquisition parameters

Parameter	Magnetic resonance imaging sequences							
	T2 FSE sagittal	T2 FSE axial	T2 FSE coronal	T1 FSE axial	DWI axial	T1 + GD axial	T1 + GD coronal	T1 + GD coronal
Repetition time in ms	5325	9890	7509	850	7750	435	295	265
Echo time in ms	102	102	102	Min	Min	Min	Min	Min
Slices, *n*	30	40	30	40	40	40	40	30
FOV	24	20	20	20	20	20	20	24
Slices thickness in mm	4	4	4	4	4	4	4	4
Broadband in Hz/Px	62.5	62.5	50	62.5	-	50	50	50
Phase	384	384	416	384	60	320	320	320
Acquisition time in min:s	2:35	3:08	2:45	3:53	5:18	2:31	2:16	2:02

DWI: Diffusion-weighted imaging; FSE: Fast spin-echo; GD: Gadolinium; MRI: Magnetic resonance imaging.

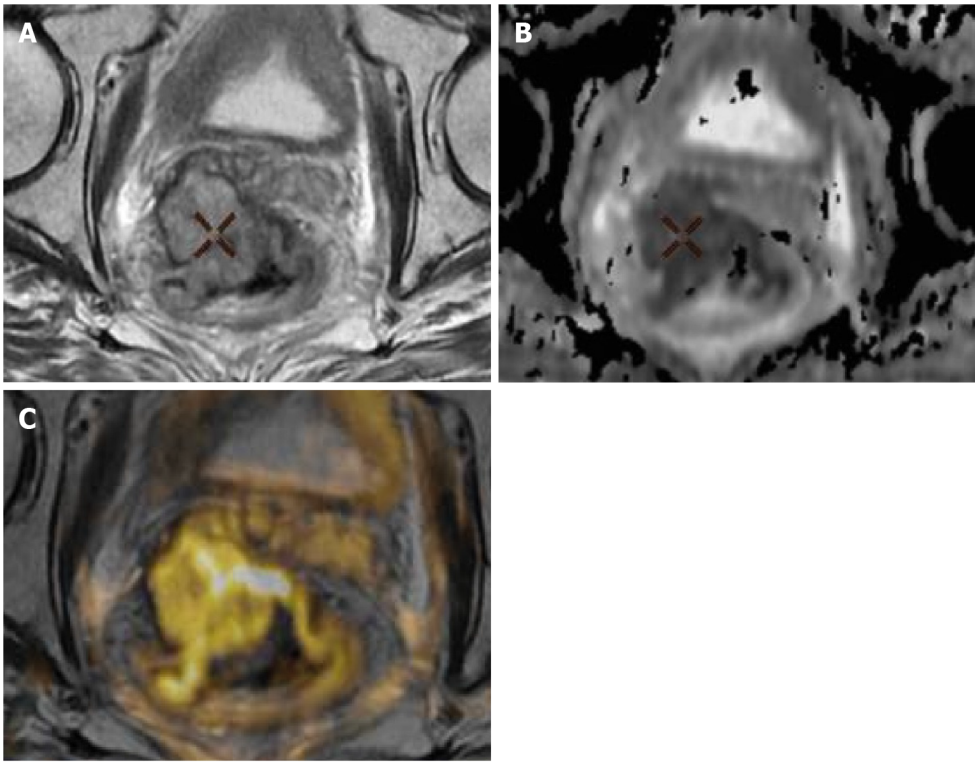

DOI: 10.3748/wjg.v28.i23.2609

Figure 1 Representative images of magnetic resonance imaging protocol. A-C: Axial T2 (A), apparent diffusion coefficient (ADC) map and T2 fusion ADC map color (B) and images of bulky tumor (C), showing tumor extending more than 5 mm into the mesorectal fat and invading the mesorectal fascia.

It should be noted that, in the first instance, one large ROI was placed to cover most of the largest axial tumor cross-section, which facilitated the calculation of the ADCmean values (ROI ADCmean). Thereafter, a volume of interest (VOI) was manually created on the ADC maps, where ROIs were drawn on all tumor slices (whole-lesion measurement). Within this VOI, the following parameters were calculated: (1) ADCmean, the average ADC value of all voxels within the VOI; (2) ADCn% (10^{th}, 25^{th}, 50^{th}, 75^{th}, and 90^{th} percentiles), the point at which the n% of the voxel values that formed the histogram were found to be at the left; (3) skewness, which measures the asymmetry of the distribution of values about the mean value; and (4) kurtosis, which is a measure of the 'peakedness' of the distribution of values in the ROI image. The corresponding frequency table for each lesion was exported, and the histogram parameters were computed by SPSS v. 26.0 (IBM Corporation, Armonk, NY, United States). Figure 2 is a schematic illustration of a representative ROI.

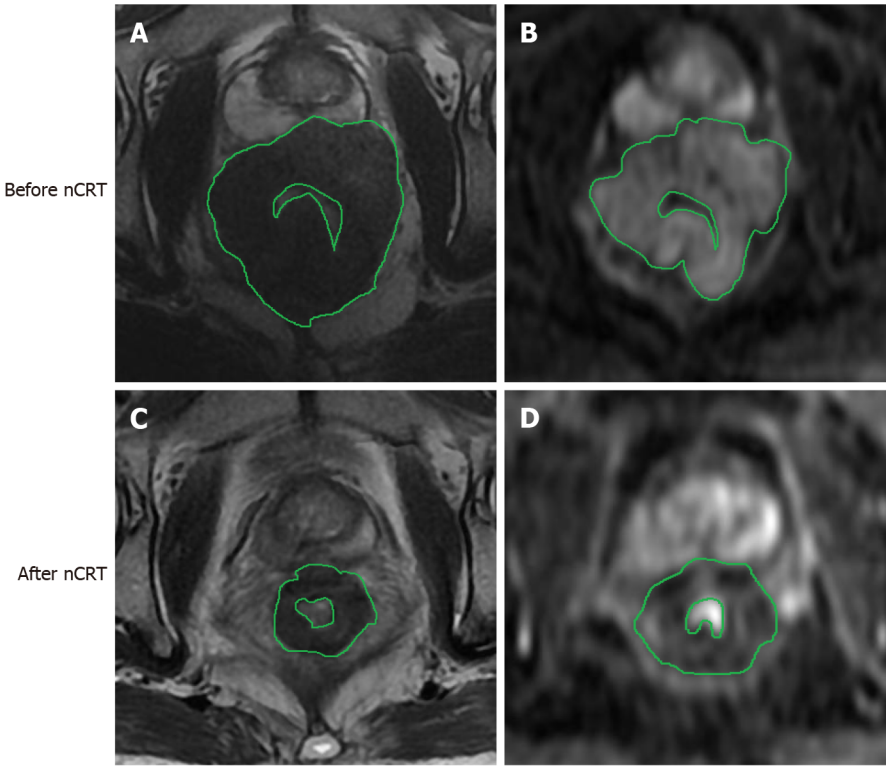

DOI: 10.3748/wjg.v28.i23.2609

Figure 2 Images of rectal tumor before and after neoadjuvant chemoradiation therapy. A, C: T2-weighted magnetic resonance images obtained in 67-year-old man with a rectal tumor (histopathologic response Ryan 1) to evaluate tumor volume; B, D: Diffusion-weighted images (DWI) that were obtained from the same case. As we can see in the present case, regions of interest were drawn manually slice by slice on DWI images along the edge of the lesion to cover as much tumor area as possible without excluding cystic or necrotic areas. nCRT: Neoadjuvant chemoradiation therapy.

Histopathologic review

Specimens were evaluated according to an established protocol that was previously described by our research team[26]. In brief, fresh surgical specimens were evaluated to determine the quality of the mesorectal excision before being fixed in 4% formaldehyde for 48 h prior to sectioning. After fixation, the specimens were serially sectioned (in slices of 1 cm), and the mesorectal boundary was linked. When the residual tumor was visible, a minimum submission of four blocks was recommended. All mesorectal lymph nodes were histologically examined, as was the involvement of the circumferential resection margin. When no residual tumor cells were identified, each block was cut into 3 level sections, and immuhistochemistry for keratin was done. All hematoxylin and eosin slides were reviewed by an experienced pathologist (EHB, with 15 years of experience examining rectal cancer).

The pathologic response of the primary tumor was estimated using the modified Ryan's classification as follow[26,27]: TRG0, complete response with no viable cancer cells; TRG1 moderate response with single cancer cells or small groups of cancer cells; TRG2, minimal response with residual cancer outgrown by fibrosis, and TRG3, poor response with minimal or no tumor killing and extensive residual cancer.

Statistical analyses

The following formula was used to calculate changes in all metrics included in the current study: *PerC* = (Parameter post-treatment - Parameter pre-treatment) / Parameter pre−treatment × 100.

It must be noted that when pre- and post-nCRT kurtosis values were obtained, a result of +3.00 indicated the absence of kurtosis. To simplify the interpretation, we adjusted this result to 0 (*i.e.* kurtosis of –3 = 0). Thus, any reading other than 0 was referred to as an excess of kurtosis. On the other side, to negate division by 0 when calculating the percentage change in kurtosis, we added 3, *i.e.* [(Kurtosis post-treatment + 3) – (Kurtosis pre-treatment + 3) / (Kurtosis pre-treatment + 3)] × 100.

In the case of skewness, and to avoid dividing by 0, only change (not the percentage change) was used (*i.e.* skewness post treatment – skewness pre-treatment)[28]. As skewness did not have a lower bound such as kurtosis, the +/– sign was considered to calculate changes in this parameter. To compare variables among R and non-R, a Mann–Whitney *U* test (MWU) was applied, as the Kolmogorov-Smirnov test confirmed the non-normal distribution of any parameter included here. Accordingly, the data were presented as medians and interquartile ranges (IQR)[29]. When the differences in a variable were significant ($P < 0.05$) in the MWU test, the cut-off value, sensitivity, specificity, positive predictive

value, negative predictive value, area under the receiver operating characteristic (ROC) curve (AUC), and accuracy, were analyzed. The optimal cut-off values of ADCmean from the hot spot ROI and parameters derived from the histogram analysis of DWI were determined *via* the Youden index, while differences in the AUC were analyzed according to the method described by DeLong *et al*[30]. Furthermore, the diagnostic odd ratio (DOR) was designed to provide an additional measure of the performance of our potentially useful biomarkers to predict treatment response in LARC.

Finally, the intraobserver variability and interobserver variability were assessed using the intraclass correlation coefficient (ICC). For the agreement analysis, the outcomes were interpreted as follows, in accordance with Cicchetti (1994): 0.2 or less, poor agreement; 0.21–0.40, fair agreement; 0.41–0.60, moderate agreement; 0.61–0.74, good agreement; and 0.75–1.00, excellent agreement[31]. Statistical analyses were performed using SPSS v. 26. $P < 0.05$ was considered statistically significant.

RESULTS

Among the 58 patients that were originally included in this study, 10 had severe imaging artifacts. Thus, our final sample included 48 patients whose clinical and pathological characteristics are described in Table 2.

The median values and IQRs for the ROI ADCmean values and parameters derived from the histogram analysis of DWI are described in Table 3. Accordingly, post-nCRT kurtosis, as well as post-nCRT skewness, were significantly lower in R than in non-R (both $P < 0.001$, respectively). Furthermore, our results showed significant differences in the relative changes of kurtosis (Δ%kurtosis) between R and non-R ($P < 0.001$), with the largest loss of kurtosis in R. Additionally, median Δskewness displayed lower values in R than in non-R ($P < 0.001$).

We also found that patients with a favorable response (R) had higher post-nCRT ADC10th values than did non-R ($P = 0.036$). Correspondingly, the median values of Δ%ADC10th, Δ%ADCmean, and ROI Δ%ADCmean were also higher in R than in non-R, ($P = 0.020$, $P = 0.032$ and $P = 0.020$, respectively).

Receiver operating characteristics of those parameters that exhibited significant differences in the MWU test are reported in Table 4. The highest AUC values for predicting the treatment response in LARC were demonstrated by Δ%kurtosis, post-nCRT kurtosis, Δskewness and post-nCRT skewness (AUCs = 0.991, 0.985, 0.885, and 0.815, respectively). Meanwhile, the lowest diagnostic accuracy was observed in post-nCRT ADC10th (AUC = 0.681), Δ%ADCmean (AUC = 0.686), Δ%ADC10th (AUC = 0.589) and ROI Δ%ADCmean (AUC = 0.583).

The ROC curves for Δ%kurtosis, post-nCRT kurtosis, Δskewness, and post-nCRT skewness are displayed in Figure 3, while the comparison of AUC values between all of our potentially useful biomarkers for predicting the treatment response in LARC are presented in Supplementary Table 1.

It is important to mention that according to the DeLong analysis, no significant differences were found in the diagnostic accuracy of Δ%kurtosis and post-nCRT kurtosis. As well, no differences were demonstrated between Δskewness and post-nCRT skewness. However, the latter two parameters had lower accuracy than kurtosis-derivate metrics.

Finally, to verify the diagnostic accuracy of all metrics reported in Table 4, we calculated DORs. The DOR of a test is the ratio of the odds of positivity if a patient has a disease relative to the odds of positivity when a patient does not have a disease. The value of DOR ranges from 0 to infinity, with higher values indicating better discriminatory test performance[32,33]. As demonstrated in Table 5, Δ%kurtosis and post-nCRT kurtosis had the highest power of discrimination for treatment response by using DORs (approximately 376), followed by Δskewness (192.2) and post-nCRT skewness (168.6). Meanwhile, the lowest power of discrimination was observed in post-CRT ADC10th (5.48), Δ%ADCmean (4.26), Δ%ADC10th (3.65), and ROI Δ%ADCmean (3.47).

Regarding interobserver and intraobserver variability, the parameters derived from the histogram analysis of DWI, as well as the ADC values from the hotspot ROI, had an excellent agreement. The ICC measuring intraobserver variability ranges from 0.777-0.931 (Table 6), while the ICC measuring intraobserver variability ranges from 0.889-0.993 (Table 7).

DISCUSSION

Heterogeneity of malignant lesions is a feature that can be determined by characterizing changes in the histogram analysis of ADC values, which is recognized as a promising tool in cancer research when discerning between benign and malignant tumors or to better characterize the response to anti-cancer treatments[34-38].

This study focused on the ADCmean from the hot-spot ROI and a series of parameters corresponding to certain points on the ADC histogram using DWI, which have been proposed to predict treatment response in patients with rectal cancer[39,40]. As our results demonstrated, the parameters that changed significantly in response to nCRT were Δ%kurtosis, post-nCRT kurtosis, Δskewness, post-nCRT skewness, post-nCRT ADC10th, Δ%ADCmean, Δ%ADC10th, and ROI Δ%ADCmean. However, the

Table 2 Clinical and pathological characteristics of the patients' studies

Characteristics	*n* (%)
Sex	
Female	23 (48)
Male	25 (52)
RECIST 1.1	
Partial response	22 (46)
Stable disease	13 (27)
Progressive disease	13 (27)
Ryan's classification	
0	18 (38)
1	10 (21)
2	9 (19)
3	11 (22)
Treatment response	
Complete responders after nCRT	18 (38)
Non-responders' patients after nCRT	30 (62)
Tumor location	
Upper third	7 (15)
Middle third	14 (29)
Lower third	20 (41)
Diffuse	7 (15)
ypT stage	
T0	4 (8)
T1s	4 (8)
T1a	2 (4)
T2	8 (17)
T3	20 (42)
T4b	10 (21)
ypN stage	
N0	20 (42)
N1a	14 (29)
Nic	14 (29)
Degree of differentiation	
Well-differentiated adenocarcinoma	6 (13)
Moderately differentiated adenocarcinoma	35 (73)
Poorly differentiated adenocarcinoma	7 (14)
Surgical approach	
Low anterior resection	16 (33)
Intersphincteric resection	26 (54)
Abdominoperineal resection	6 (13)

nCRT: Neoadjuvant chemoradiation therapy.

Table 3 Median and interquartile range of pre- and post-neoadjuvant chemoradiation therapy parameters, as well as of changes between pre- and post-treatment values

	Responders	Non-responders	*P* value
Pre-nCRT parameters			
pre-nCRT ADCmean	0.75 (0.60-0.90)	0.85 (0.70-0.90)	0.146
10^{th} percentile	0.20 (0.17-0.23)	0.20 (0.17-0.26)	0.812
25th percentile	0.32 (0.29-0.35)	0.32 (0.23-0.41)	1.000
50^{th} percentile	0.40 (0.35-0.40)	0.40 (0.30-0.50)	0.698
75^{th} percentile	0.56 (0.47-0.58)	0.57 (0.45-0.63)	0.391
90^{th} percentile	0.71 (0.55-0.77)	0.76 (0.50-0.80)	0.556
Skewness	1.10 (0.90-1.14)	1.19 (0.88-1.37)	0.135
Kurtosis	0.89 (0.83-0.92)	0.92 (0.83-0.95)	0.296
ROI ADCmean	0.92 (0.80-1.20)	0.91 (0.83-0.93)	0.562
Post- nCRT parameters			
post- nCRT ADC_{mean}	1.20 (0.98-1.52)	1.10 (0.90-1.30)	0.065
10^{th} percentile	0.36 (0.30–0.37)	0.32 (0.31–0.34)	0.036[1]
25^{th} percentile	0.41 (0.40-0.52)	0.42 (0.41-0.50)	0.476
50^{th} percentile	0.66 (0.56-0.70)	0.65 (0.51-0.66)	0.127
75^{th} percentile	0.71 (0.67-0.80)	0.70 (0.66-0.75)	0.050
90^{th} percentile	0.89 (0.80-0.95)	0.80 (0.79-0.89)	0.105
Skewness	0.92 (0.60–1.14)	2.00 (1.15–2.67)	< 0.001[1]
Kurtosis	0.65 (0.59–0.72)	0.90 (0.80–0.90)	< 0.001[1]
ROI ADCmean	2.50 (1.50-2.70)	2.00 (1.80-2.30)	0.056
Changes between pre-treatment and post-treatment			
Δ%ADCmean	57% (14%–103%)	27% (0%–59%)	0.032[1]
Δ%$ADC10^{th}$	86% (37%–118%)	48% (11%–88%)	0.020[1]
Δ%$ADC25^{th}$	39% (19%-57%)	22% (0%-58%)	0.905
Δ%$ADC50^{th}$	70% (31%-86%)	31% (2%-65%)	0.067
Δ%$ADC75^{th}$	40% (20%-61%)	37% (0%-57%)	0.288
Δ%$ADC90^{th}$	27% (11%-58%)	9% (7%-119%)	0.061
Δskewness	–0.20 (–0.40–0.00)	0.49 (0.10–0.50)	< 0.001[1]
Δ%kurtosis	41% (18%–54%)	2.5% (1.4%–5.9%)	< 0.001[1]
ROI Δ%ADCmean	55% (48%–60%)	23% (15%–30%)	0.020[1]

[1]Statistically significant difference. ADC: Apparent diffusion coefficient; nCRT: Neoadjuvant chemoradiation therapy; ROI: Region of interest.

highest diagnostic accuracy was obtained for Δ%kurtosis, post-nCRT kurtosis, post-nCRT skewness, and Δskewness, suggesting that these metrics might be useful when selecting responders (TRG 0) for an organ preservation approach with either 'watch-and-wait' or local excision[39,40].

The results derivate from parameters with the highest diagnostic accuracy in predicting treatment response to nCRT in the current work are reviewed below.

First, we demonstrated that both post-nCRT kurtosis and post-nCRT skewness were significantly lower in R than in non-R. The overall trends from the histogram studies have shown that, following treatment, the histogram analysis of *DWI* and diffusion kurtosis imaging (DKI) shifted to the right upon decreased kurtosis and skewness in rectal cancer[39-43]. For example, in 2017, Hu *et al*[39] reported that the post-treatment mean kurtosis derived from DKI showed reduced values in R when compared with non-R patients, whereas Enkhbaatar *et al*[23] (2019) documented that the histogram of R presented negative changes in skewness following a loss of this parameter after therapy.

Table 4 Diagnostic performance of the best magnetic resonance imaging histogram derived parameters to detect responder patients

	Cutoff	Sensitivity	Specificity	PPV	NPV	Accuracy	AUC (95%CI)
Δ%kurtosis	11.85%	94.4%	96.7%	94.4%	96.7%	96.0%	0.991 (0.925-1.000)
Post-nCRT kurtosis	0.78	93.3%	99.0%	90%	99.0%	96.0%	0.985 (0.957-1.000)
Δskewness	0.16	66.7%	99.0%	64.3%	99.0%	79.2%	0.885 (0.795-0.975)
Post-nCRT skewness	1.59	63.3%	99.0%	62.0%	99.0%	77.1%	0.815 (0.795-0.634)
Post-nCRT ADC10th	0.34×10^{-3} mm^2/s	66.7%	73.3%	60.0%	79.0%	71.0%	0.681 (0.509-0.852)
Δ%ADCmean	56.00%	56.0%	77.0%	56.0%	73.3%	66.7%	0.686 (0.500-0.820
Δ%ADC10th	74.21%	61.1%	70.0%	55.0%	75.0%	66.7%	0.589 (0.483-0.815)
ROI Δ%ADCmean	55.00%	61.0%	69.0%	52.0%	72.0%	65.3%	0.583 (0.425-0.715)

ADC: Apparent diffusion coefficient; AUC: Area under the receiver operating characteristic curve; nCRT: Neoadjuvant chemoradiation therapy; NPV: Negative predictive value; PPV: Positive predictive value; ROI: Region of interest.

Table 5 Diagnostic odds ratios of magnetic resonance imaging parameters in differentiating respond and non- respond patients in locally advanced rectal cancer

	Diagnostic odds ratio	95%CI
Δ%kurtosis	376.0	228.9-842.1
Post-nCRT kurtosis	375.3	225.7-887.7
Δskewness	192.2	69.0-253.3
Post-nCRT skewness	168.6	54.0-251.7
Post-nCRT ADC10th	5.48	1.0-19.6
Δ%ADCmean	4.26	1.0-14.4
Δ%ADC10th	3.65	1.0-12.5
ROI Δ%ADCmean	3.47	1.0-11.2

ADC: Apparent diffusion coefficient; nCRT: Neoadjuvant chemoradiation therapy; ROI: Region of interest.

In the same way, kurtosis from R had greater reductions than from non-R, which indicates Gaussian or flatter distributions in patients with a complete response to the therapy. In biological tissues, it is believed that the non-Gaussian behavior (more precisely, a platykurtic curve) of water might occur because of a heterogeneous environment characterized by multiple compartments, organelles, and semipermeable membranes[44]. Thus, when an important reduction in kurtosis is noticed, a higher displacement of water molecules in DWI is assumed.

Furthermore, as mentioned above, negative changes of skewness after nCRT were seen in R, while non-R exhibited positive changes in this parameter. Negatively skewed curves show the majority of scores above the mean, and positively skewed curves are just the opposite[44]. In physiology, the association between changes in skewness and responses to antineoplastic therapy have not been fleshed out, but a curve negatively skewed suggests a loss of cellular structure[23]. Therefore, favorable treatment response is suspected.

Our MWU analysis also found differences between R and non-R across other parameters, such as ADC10th, Δ%ADCth, Δ%ADCmean and ROIΔ%ADCmean, as stated in our results section. However, both the ROC curve analysis and the DOR calculation indicated that only Δ%kurtosis, post-nCRT kurtosis, Δskewness, and post-nCRT skewness appear to predict a favorable response to the therapy, whereas the other metrics did not possess that predictive property.

Briefly, the Youden index calculation indicated that post-nCRT kurtosis, post-nCRT skewness, and Δskewness values below 0.78×10^{-3} mm^2/s, 1.59×10^{-3} mm^2/s, and 0.16, respectively, might be significant indicators of the occurrence of pCR. Meanwhile, Δ% changes above 11.85% also indicated a positive treatment effect with high accuracy. It is important to remember that, according to the DeLong analysis, the kurtosis-related parameters exhibit a better diagnostic performance than do skewness-related parameters.

Table 6 Intraobserver variability

		ICC	95%CI
Basal			
Test1 and test2, reader1	ROI ADCmean	0.850	0.742–0.800
Test1 and test2, reader2	ROI ADCmean	0.890	0.850-0.820
After treatment			
Test1 and test2, reader1	ROI ADCmean	0.800	0.750-0.819
Test1 and test2, reader2	ROI ADCmean	0.823	0.800-0.850
Basal			
Test1 and test2, reader1	ADCmean	0.850	0.756-0.920
Test1 and test2, reader2	ADCmean	0.777	0.745-0.812
After treatment			
Test1 and test2, reader1	ADCmean	0.845	0.830-0.850
Test1 and test2, reader2	ADCmean	0.823	0.800-0.833
Basal			
Test1 and test2, reader1	10^{th} percentile	0.820	0.880-0.950
Test1 and test2, reader2	10^{th} percentile	0.880	0.800-0.920
After treatment			
Test1 and test2, reader1	10^{th} percentile	0.780	0.740-0.853
Test1 and test2, reader2	10^{th} percentile	0.853	0.723-0.901
Basal			
Test1 and test2, reader1	25^{th} percentile	0.803	0.800-0.922
Test1 and test2, reader2	25^{th} percentile	0.863	0.801-0.895
After treatment			
Test1 and test2, reader1	25^{th} percentile	0.788	0.750-0.837
Test1 and test2, reader2	25^{th} percentile	0.820	0.780-0.846
Basal			
Test1 and test2, reader1	50^{th} percentile	0.850	0.840-0.920
Test1 and test2, reader2	50^{th} percentile	0.845	0.790-0.860
After treatment			
Test1 and test2, reader1	50^{th} percentile	0.821	0.800-0.913
Test1 and test2, reader2	50^{th} percentile	0.833	0.800-0.897
Basal			
Test1 and test2, reader1	75^{th} percentile	0.821	0.790-0.860
Test1 and test2, reader2	75^{th} percentile	0.859	0.820-0.920
After treatment			
Test1 and test2, reader1	75^{th} percentile	0.851	0.790-0.880
Test1 and test2, reader2	75^{th} percentile	0.837	0.791-0.856
Basal			
Test1 and test2, reader1	90^{th} percentile	0.850	0.820-0.890
Test1 and test2, reader2	90^{th} percentile	0.880	0.850-0.960
After treatment			
Test1 and test2, reader1	90^{th} percentile	0.831	0.800-0.902

Test1 and test2, reader2	90th percentile	0.901	0.850-0.975
Basal			
Test1 and test2, reader1	Skewness	0.920	0.900-0.940
Test1 and test2, reader2	Skewness	0.901	0.880-0.923
After treatment			
Test1 and test2, reader1	Skewness	0.931	0.920-0.950
Test1 and test2, reader2	Skewness	0.889	0.877-0.910
Basal			
Test1 and test2, reader1	Kurtosis	0.920	0.890-0.950
Test1 and test2, reader2	Kurtosis	0.910	0.850-0.960
After treatment			
Test1 and test2, reader1	Kurtosis	0.890	0.850-0.960
Test1 and test2, reader2	Kurtosis	0.880	0.840-0.982

ADC: Apparent diffusion coefficient; ICC: Intraclass correlation coefficient; ROI: Region of interest.

Table 7 Interobserver variability (intraclass correlation coefficient and 95% confidence intervals)

Pre-treatment	Reader one *vs* reader two	Post-treatment	Reader one *vs* reader two
ROI ADCmean	0.985 (1.900-0.999)	ROI ADCmean	0.889 (0.850-0.950)
ADCmean	0.989 (0.980–0.994)	ADCmean	0.990 (0.985-0.995)
10th percentile	0.972 (0.951–0.984)	10th percentile	0.992 (0.986–0.996)
25th percentile	0.970 (0.947–0.983)	25th percentile	0.950 (0.940-0.982)
50th percentile	0.986 (0.976–0.992)	50th percentile	0.987 (0.945-0.995)
75th percentile	0.989 (0.980–0.994)	75th percentile	0.990 (0.982–0.994)
90th percentile	0.989 (0.980–0.994)	90th percentile	0.972 (0.987–0.996)
Skewness	0.990 (0.982–0.994)	Skewness	0.993 (0.987–0.996)
Kurtosis	0.992 (0.986–0.995)	Kurtosis	0.972 (0.951–0.984)

ADC: Apparent diffusion coefficient; ROI: Region of interest.

Aligned with this finding, numerous authors have documented that kurtosis is more directly correlated to the underlying structural, physiological, molecular, and metabolic changes that occur during tumor progression than skewness[45]. This may be the reason why the kurtosis of ADC values has been used to indicate deviations from Gaussianity, even in the most challenging mathematical designs that predict the response to chemotherapy, such as radiomics analysis[46-48].

The results obtained from the ROC curved are partially supported by the estimated DORs, which were approximately 376 for both Δ%kurtosis and post-nCRT kurtosis. This means that for the cut-off points of Δ%kurtosis and post-nCRT kurtosis calculated here, the odds for positivity among subjects with a non-pCR was 376 times higher than the odds for positivity among subjects with a pCR. In the same way, Δskewness and post-nCRT skewness demonstrated respectable diagnostic performances with DOR values of 192.17 and 168.56, respectively. Although these values appear to be lower than DORs of Δ%kurtosis and post-nCRT kurtosis, the confidence intervals for these metrics clearly overlap, so we cannot conclude that the kurtosis-related parameters were statistically better than the skewness-related parameters using DOR.

Finally, this study confirm that ADC histogram analysis is a reproducible technique. Similarly, van Heeswijk *et al*[49] demonstrated that histogram-derived parameters had good interobserver agreement, with ICC values ranging from 0.80-0.98. This result supports the method's validity and suggests that it can be used in clinical practice. Furthermore, we utilized non-precise tumor delineation, which was quicker and produced comparable findings to those obtained by an expert radiologist's measurement, suggesting that this technique could be performed semiautomatically with an excellent interobserver agreement. This finding is very important when considering the implementation of histogram analysis

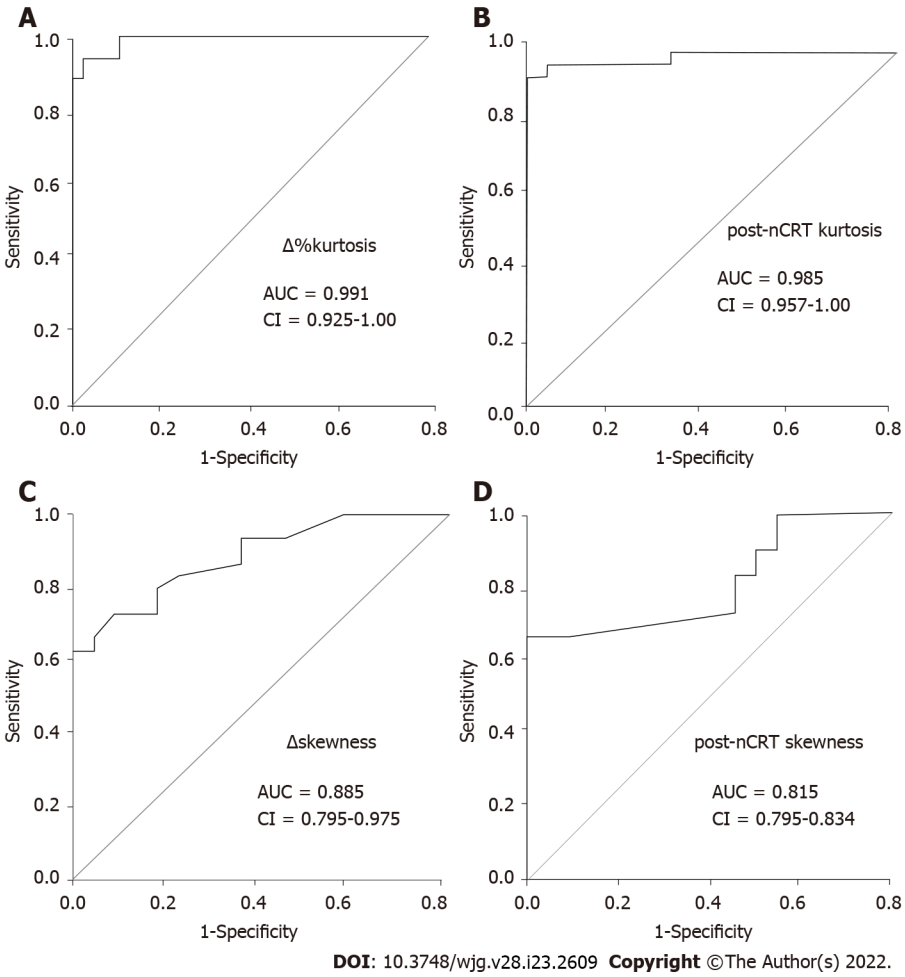

DOI: 10.3748/wjg.v28.i23.2609

Figure 3 Receiver operating characteristic curves displaying the diagnostic performances of the four histogram parameters derived from apparent diffusion coefficient values with the highest accuracy. A: Δ%kurtosis; B: Post-neoadjuvant chemoradiation therapy (nCRT) kurtosis; C: Δskewness; D: Post-nCRT skewness. AUC: Area under the receiver operating characteristic curve.

in routine clinical practice.

Our study had important limitations. First, this was a retrospective, single-center evaluation. We believe that the present study might serve as a foundation for larger prospective studies in the future. Second, we included only a small number of patients (n = 48), while no validation group was included (both restricting the conception of a predictive model by using a multivariate logistic regression analysis). Third, the patient numbers among the different histopathologic TRGs were not well balanced. Only 18 patients (38%) achieved a histopathologic complete response, which may have introduced an element of statistical bias. However, these patients achieved a strict pCR, underlying the high degree of accuracy of our metrics. Fourth, the parameters obtained from the hotspot ROI were not conclusive enough to predict treatment response in the present study. This result is still in significant disagreement with our prior work where we demonstrated a high diagnostic accuracy of the Δ%ADCmean when distinguishing a pCR in rectal cancer by choosing a cutoff value of 55%[26]. Differences in research methods might explain this discrepancy, but we sustain that it is more reliable to use volumetric ROIs than one slice ROIs.

In summary, although further studies are needed to address the limitations of the current work, we demonstrated the benefits of considering measures other than the ROI ADCmean to evaluate the response to therapy in patients with LARC. Moreover, kurtosis and skewness have been selected by many radiomics studies of rectal cancer, emphasizing the importance of first-order statistics features for the assessment of therapy response[47,50]. Our results support the importance of these parameters, but they also helped us to standardize both the extraction and analysis of the data collected, which is a crucial step when developing and validating our own multiparametric model to predict treatment outcomes.

CONCLUSION

Based on the DWI technique, some whole-lesion histogram parameters could provide valuable information when diagnosing rectal cancer. In particular, kurtosis and skewness might be a useful indicator in the preoperative evaluation of a pCR in rectal cancer. Understanding skewness and kurtosis of the ADC parameters is the simplest way to recognize the deviation of Gaussianity, which indicates tumor heterogeneity. Moreover, we demonstrated high interobserver reliability for measurements of all of the histogram-derived parameters analyzed in the current work, addressing the challenges associated with replication that are well-known among more complex predictive models. Further long-term studies are needed to determine the ultimate clinical utility of our results.

ARTICLE HIGHLIGHTS

Research background

Studies have shown that successful treatment of many tumors can be detected using diffusion-weighted magnetic resonance imaging (MRI) as an increase in the apparent diffusion coefficient (ADC). However, findings from rectal cancer have been limited. Therefore, the criteria used for tumor staging and surveillance are largely based on anatomic criteria at this time. Broadly, whole lesion histogram analysis of ADC aims to fill this gap, extracting and analyzing the higher quantitative data with the aim of more accurate, tumor-specific evaluation and characterization.

Research motivation

ADC histogram parameters reflect the distribution and variation of all voxels within the entire lesion, which reduce the subjectivity of region of interest (ROI) placement and improves repeatability in the quantitative ADC analysis. Previous studies have applied volumetric ADC histogram analysis to predict treatment response of squamous carcinoma, breast cancers, and ovarian cancers. No ADC histogram study thus far has focused on locally advanced rectal cancer (LARC).

Research objectives

We aim to evaluate the effectiveness of whole lesion histogram analysis of ADC in the prediction to neoadjuvant chemoradiation therapy (nCRT) response in patients with LARC.

Research methods

This was a retrospective study. We collected data of 48 consecutive patients with histologically confirmed LARC. All patients underwent a pre-treatment MRI for primary tumor staging and a second restaging MRI for response evaluation. The sample was distributed as follows: responders (R), n = 18; and non-responders (non-R), n = 30. Eight parameters derived from the histogram analysis of ADC, as well as the ADCmean from the hot spot ROI, were obtained and compared between R and non-R. The diagnostic accuracy in the prediction of treatment response of all variables included in the present study was calculated as well.

Research results

Post-nCRT kurtosis, Δ%kurtosis, post-nCRT skewness an Δskewness exhibited the highest diagnostic performance in predicting a good response to nCRT.

Research conclusions

The results of our study support that histogram-parameters derived from ADC values can be used to stratify good responders into studies exploring individualized, less extensive treatment regimens, such as the omission of radiotherapy and less extensive surgery, or even deferral of surgery.

Research perspectives

We need to expand the sample size to confirm further the diagnostic accuracy of kurtosis and skewness. In addition, the long-term outcome of this analysis should be a radiomic model for predict treatment response in rectal cancer.

FOOTNOTES

Author contributions: Sollozo-Dupont I designed the study; Sollozo-Dupont I and Domínguez Osorio V analyzed the data; Domínguez Osorio V and Vela-Sarmiento I collected the data; Sollozo-Dupont I, Jiménez de los Santos ME, and Reyes-Pérez JA wrote the paper; Villaseñor-Navarro Y and Moreno-Astudillo L reviewed the study; Jiménez de los Santos ME and Reyes-Pérez JA contributed equally to this work; All authors contributed to the manuscript for

important intellectual content and approved the submission.

Institutional review board statement: The study protocol was approved by the Institutional Review Board of the National Cancer Institute from México, city, and was in accordance with the Declaration of Helsinki (Approval No. 2021/026).

Informed consent statement: Patients were not required to give informed consent to the study because the analysis used anonymous clinical data that were obtained after each patient agreed to treatment by written consent.

Conflict-of-interest statement: The authors have no conflicts of interest to declare.

Data sharing statement: The raw data supporting the conclusions of this article will be made available by the authors.

Country/Territory of origin: Mexico

ORCID number: Mayra Evelia Jiménez de Los Santos 0000-0003-1350-4761; Juan Armando Reyes-Pérez 0000-0002-1519-3613; Victor Domínguez Osorio 0000-0001-8660-7994; Yolanda Villaseñor-Navarro 0000-0001-5065-7922; Liliana Moreno-Astudillo 0000-0003-3125-708X; Itzel Vela-Sarmiento 0000-0002-6516-4212; Isabel Sollozo-Dupont 0000-0002-4569-3643.

S-Editor: Wang JL
L-Editor: Filipodia
P-Editor: Wang JL

REFERENCES

1 **Chen M**, Chen LZ, Xu L, Zhang JS, Song X. Neoadjuvant chemoradiation for locally advanced rectal cancer: a systematic review of the literature with network meta-analysis. *Cancer Manag Res* 2019; **11**: 741-758 [PMID: 30697067 DOI: 10.2147/CMAR.S189445]
2 **Ryan ÉJ**, Creavin B, Sheahan K. Delivery of Personalized Care for Locally Advanced Rectal Cancer: Incorporating Pathological, Molecular Genetic, and Immunological Biomarkers Into the Multimodal Paradigm. *Front Oncol* 2020; **10**: 1369 [PMID: 32923389 DOI: 10.3389/fonc.2020.01369]
3 **Curvo-Semedo L**, Lambregts DM, Maas M, Thywissen T, Mehsen RT, Lammering G, Beets GL, Caseiro-Alves F, Beets-Tan RG. Rectal cancer: assessment of complete response to preoperative combined radiation therapy with chemotherapy--conventional MR volumetry versus diffusion-weighted MR imaging. *Radiology* 2011; **260**: 734-743 [PMID: 21673229 DOI: 10.1148/radiol.11102467]
4 **Spring LM**, Fell G, Arfe A, Sharma C, Greenup R, Reynolds KL, Smith BL, Alexander B, Moy B, Isakoff SJ, Parmigiani G, Trippa L, Bardia A. Pathologic Complete Response after Neoadjuvant Chemotherapy and Impact on Breast Cancer Recurrence and Survival: A Comprehensive Meta-analysis. *Clin Cancer Res* 2020; **26**: 2838-2848 [PMID: 32046998 DOI: 10.1158/1078-0432.CCR-19-3492]
5 **Chen W**, Mao L, Li L, Wei Q, Hu S, Ye Y, Feng J, Liu B, Liu X. Predicting Treatment Response of Neoadjuvant Chemoradiotherapy in Locally Advanced Rectal Cancer Using Amide Proton Transfer MRI Combined With Diffusion-Weighted Imaging. *Front Oncol* 2021; **11**: 698427 [PMID: 34277445 DOI: 10.3389/fonc.2021.698427]
6 **Chen L**, Liu M, Bao J, Xia Y, Zhang J, Zhang L, Huang X, Wang J. The correlation between apparent diffusion coefficient and tumor cellularity in patients: a meta-analysis. *PLoS One* 2013; **8**: e79008 [PMID: 24244402 DOI: 10.1371/journal.pone.0079008]
7 **Vossen JA**, Buijs M, Geschwind JF, Liapi E, Prieto Ventura V, Lee KH, Bluemke DA, Kamel IR. Diffusion-weighted and Gd-EOB-DTPA-contrast-enhanced magnetic resonance imaging for characterization of tumor necrosis in an animal model. *J Comput Assist Tomogr* 2009; **33**: 626-630 [PMID: 19638862 DOI: 10.1097/RCT.0b013e3181953df3]
8 **Dzik-Jurasz A**, Domenig C, George M, Wolber J, Padhani A, Brown G, Doran S. Diffusion MRI for prediction of response of rectal cancer to chemoradiation. *Lancet* 2002; **360**: 307-308 [PMID: 12147376 DOI: 10.1016/S0140-6736(02)09520-X]
9 **Lambregts DM**, Vandecaveye V, Barbaro B, Bakers FC, Lambrecht M, Maas M, Haustermans K, Valentini V, Beets GL, Beets-Tan RG. Diffusion-weighted MRI for selection of complete responders after chemoradiation for locally advanced rectal cancer: a multicenter study. *Ann Surg Oncol* 2011; **18**: 2224-2231 [PMID: 21347783 DOI: 10.1245/s10434-011-1607-5]
10 **Xie H**, Sun T, Chen M, Wang H, Zhou X, Zhang Y, Zeng H, Wang J, Fu W. Effectiveness of the apparent diffusion coefficient for predicting the response to chemoradiation therapy in locally advanced rectal cancer: a systematic review and meta-analysis. *Medicine (Baltimore)* 2015; **94**: e517 [PMID: 25674749 DOI: 10.1097/MD.0000000000000517]
11 **Tarallo N**, Angeretti MG, Bracchi E, Xhepa G, Molinelli V, Tagliaferri C, Antognoni P, Novario R, Sessa F, Fugazzola C. Magnetic resonance imaging in locally advanced rectal cancer: quantitative evaluation of the complete response to neoadjuvant therapy. *Pol J Radiol* 2018; **83**: e600-e609 [PMID: 30800199 DOI: 10.5114/pjr.2018.81156]
12 **Meng X**, Huang Z, Wang R, Yu J. Prediction of response to preoperative chemoradiotherapy in patients with locally

advanced rectal cancer. *Biosci Trends* 2014; **8**: 11-23 [PMID: 24647108 DOI: 10.5582/bst.8.11]
13 **Gu J**, Khong PL, Wang S, Chan Q, Law W, Zhang J. Quantitative assessment of diffusion-weighted MR imaging in patients with primary rectal cancer: correlation with FDG-PET/CT. *Mol Imaging Biol* 2011; **13**: 1020-1028 [PMID: 20872077 DOI: 10.1007/s11307-010-0433-7]
14 **Marzi S**, Minosse S, Vidiri A, Piludu F, Giannelli M. Diffusional kurtosis imaging in head and neck cancer: On the use of trace-weighted images to estimate indices of non-Gaussian water diffusion. *Med Phys* 2018; **45**: 5411-5419 [PMID: 30317646 DOI: 10.1002/mp.13238]
15 **Guo Y**, Kong QC, Li LQ, Tang WJ, Zhang WL, Ning GY, Xue J, Zhou QW, Liang YY, Wu M, Jiang XQ. Whole Volume Apparent Diffusion Coefficient (ADC) Histogram as a Quantitative Imaging Biomarker to Differentiate Breast Lesions: Correlation with the Ki-67 Proliferation Index. *Biomed Res Int* 2021; **2021**: 4970265 [PMID: 34258262 DOI: 10.1155/2021/4970265]
16 **Tang WJ**, Jin Z, Zhang YL, Liang YS, Cheng ZX, Chen LX, Liang YY, Wei XH, Kong QC, Guo Y, Jiang XQ. Whole-Lesion Histogram Analysis of the Apparent Diffusion Coefficient as a Quantitative Imaging Biomarker for Assessing the Level of Tumor-Infiltrating Lymphocytes: Value in Molecular Subtypes of Breast Cancer. *Front Oncol* 2020; **10**: 611571 [PMID: 33489920 DOI: 10.3389/fonc.2020.611571]
17 **Ao W**, Bao X, Mao G, Yang G, Wang J, Hu J. Value of Apparent Diffusion Coefficient for Assessing Preoperative T Staging of Low Rectal Cancer and Whether This Is Correlated With Ki-67 Expression. *Can Assoc Radiol J* 2020; **71**: 5-11 [PMID: 32063001 DOI: 10.1177/0846537119885666]
18 **Donati OF**, Mazaheri Y, Afaq A, Vargas HA, Zheng J, Moskowitz CS, Hricak H, Akin O. Prostate cancer aggressiveness: assessment with whole-lesion histogram analysis of the apparent diffusion coefficient. *Radiology* 2014; **271**: 143-152 [PMID: 24475824 DOI: 10.1148/radiol.13130973]
19 **Li HM**, Zhang R, Gu WY, Zhao SH, Lu N, Zhang GF, Peng WJ, Qiang JW. Whole solid tumour volume histogram analysis of the apparent diffusion coefficient for differentiating high-grade from low-grade serous ovarian carcinoma: correlation with Ki-67 proliferation status. *Clin Radiol* 2019; **74**: 918-925 [PMID: 31471063 DOI: 10.1016/j.crad.2019.07.019]
20 **Liu HL**, Zong M, Wei H, Wang C, Lou JJ, Wang SQ, Zou QG, Jiang YN. Added value of histogram analysis of apparent diffusion coefficient maps for differentiating triple-negative breast cancer from other subtypes of breast cancer on standard MRI. *Cancer Manag Res* 2019; **11**: 8239-8247 [PMID: 31564982 DOI: 10.2147/CMAR.S210583]
21 **Lu J**, Li HM, Cai SQ, Zhao SH, Ma FH, Li YA, Ma XL, Qiang JW. Prediction of Platinum-based Chemotherapy Response in Advanced High-grade Serous Ovarian Cancer: ADC Histogram Analysis of Primary Tumors. *Acad Radiol* 2021; **28**: e77-e85 [PMID: 32061467 DOI: 10.1016/j.acra.2020.01.024]
22 **Cho SH**, Kim GC, Jang YJ, Ryeom H, Kim HJ, Shin KM, Park JS, Choi GS, Kim SH. Locally advanced rectal cancer: post-chemoradiotherapy ADC histogram analysis for predicting a complete response. *Acta Radiol* 2015; **56**: 1042-1050 [PMID: 25270374 DOI: 10.1177/0284185114550193]
23 **Enkhbaatar NE**, Inoue S, Yamamuro H, Kawada S, Miyaoka M, Nakamura N, Sadahiro S, Imai Y. MR Imaging with Apparent Diffusion Coefficient Histogram Analysis: Evaluation of Locally Advanced Rectal Cancer after Chemotherapy and Radiation Therapy. *Radiology* 2018; **288**: 129-137 [PMID: 29558294 DOI: 10.1148/radiol.2018171804]
24 **Peng Y**, Tang H, Hu X, Shen Y, Kamel I, Li Z, Hu D. Rectal Cancer Invasiveness: Whole-Lesion Diffusion-Weighted Imaging (DWI) Histogram Analysis by Comparison of Reduced Field-of-View and Conventional DWI Techniques. *Sci Rep* 2019; **9**: 18760 [PMID: 31822707 DOI: 10.1038/s41598-019-55059-0]
25 **Peng Y**, Tang H, Meng X, Shen Y, Hu D, Kamel I, Li Z. Histological grades of rectal cancer: whole-volume histogram analysis of apparent diffusion coefficient based on reduced field-of-view diffusion-weighted imaging. *Quant Imaging Med Surg* 2020; **10**: 243-256 [PMID: 31956546 DOI: 10.21037/qims.2019.11.17]
26 **Jiménez de Los Santos ME**, Reyes-Pérez JA, Sandoval-Nava RM, Villalobos-Juárez JL, Villaseñor-Navarro Y, Vela-Sarmiento I, Sollozo-Dupont I. The apparent diffusion coefficient is a useful biomarker in predicting treatment response in patients with locally advanced rectal cancer. *Acta Radiol Open* 2020; **9**: 2058460120957295 [PMID: 32974055 DOI: 10.1177/2058460120957295]
27 **Edge SB**, Compton CC. The American Joint Committee on Cancer: the 7th edition of the AJCC cancer staging manual and the future of TNM. *Ann Surg Oncol* 2010; **17**: 1471-1474 [PMID: 20180029 DOI: 10.1245/s10434-010-0985-4]
28 **Haider MA**, Vosough A, Khalvati F, Kiss A, Ganeshan B, Bjarnason GA. CT texture analysis: a potential tool for prediction of survival in patients with metastatic clear cell carcinoma treated with sunitinib. *Cancer Imaging* 2017; **17**: 4 [PMID: 28114978 DOI: 10.1186/s40644-017-0106-8]
29 **Stroup DF**, Smith CK, Truman BI. Reporting the methods used in public health research and practice. *J Public Health Emerg* 2017; **1** [PMID: 29417955 DOI: 10.21037/jphe.2017.12.01]
30 **DeLong ER**, DeLong DM, Clarke-Pearson DL. Comparing the areas under two or more correlated receiver operating characteristic curves: a nonparametric approach. *Biometrics* 1988; **44**: 837-845 [PMID: 3203132]
31 **Cicchetti DV**. Guidelines, criteria, and rules of thumb for evaluating normed and standardized assessment instruments in psychology. *Psychol Assess* 1994; **6**: 284-290 [DOI: 10.1037/1040-3590.6.4.284]
32 **Glas AS**, Lijmer JG, Prins MH, Bonsel GJ, Bossuyt PM. The diagnostic odds ratio: a single indicator of test performance. *J Clin Epidemiol* 2003; **56**: 1129-1135 [PMID: 14615004 DOI: 10.1016/s0895-4356(03)00177-x]
33 **Chang SM**, Matchar DB, Gerald W Smetana GW, Umscheid CA. Methods Guide for Medical Test Reviews. Rockville: Agency for Healthcare Research and Quality (US), 2012 [PMID: 22834019]
34 **Le Bihan D**, Iima M. Diffusion Magnetic Resonance Imaging: What Water Tells Us about Biological Tissues. *PLoS Biol* 2015; **13**: e1002203 [PMID: 26204162 DOI: 10.1371/journal.pbio.1002203]
35 **Pyatigorskaya N**, Le Bihan D, Reynaud O, Ciobanu L. Relationship between the diffusion time and the diffusion MRI signal observed at 17.2 Tesla in the healthy rat brain cortex. *Magn Reson Med* 2014; **72**: 492-500 [PMID: 24022863 DOI: 10.1002/mrm.24921]
36 **Just N**. Improving tumour heterogeneity MRI assessment with histograms. *Br J Cancer* 2014; **111**: 2205-2213 [PMID: 25268373 DOI: 10.1038/bjc.2014.512]

37 **O'Connor JP**, Rose CJ, Waterton JC, Carano RA, Parker GJ, Jackson A. Imaging intratumor heterogeneity: role in therapy response, resistance, and clinical outcome. *Clin Cancer Res* 2015; **21**: 249-257 [PMID: 25421725 DOI: 10.1158/1078-0432.CCR-14-0990]

38 **Rosenkrantz AB**. Histogram-based apparent diffusion coefficient analysis: an emerging tool for cervical cancer characterization? *AJR Am J Roentgenol* 2013; **200**: 311-313 [PMID: 23345351 DOI: 10.2214/AJR.12.9926]

39 **Hu F**, Tang W, Sun Y, Wan D, Cai S, Zhang Z, Grimm R, Yan X, Fu C, Tong T, Peng W. The value of diffusion kurtosis imaging in assessing pathological complete response to neoadjuvant chemoradiation therapy in rectal cancer: a comparison with conventional diffusion-weighted imaging. *Oncotarget* 2017; **8**: 75597-75606 [PMID: 29088894 DOI: 10.18632/oncotarget.17491]

40 **Xie H**, Wu G. Application of Diffusion Kurtosis Imaging and Histogram Analysis for Assessing Preoperative Stages of Rectal Cancer. *Gastroenterol Res Pract* 2018; **2018**: 9786932 [PMID: 29967642 DOI: 10.1155/2018/9786932]

41 **Sun YS**, Zhang XP, Tang L, Ji JF, Gu J, Cai Y, Zhang XY. Locally advanced rectal carcinoma treated with preoperative chemotherapy and radiation therapy: preliminary analysis of diffusion-weighted MR imaging for early detection of tumor histopathologic downstaging. *Radiology* 2010; **254**: 170-178 [PMID: 20019139 DOI: 10.1148/radiol.2541082230]

42 **Traverso A**, Kazmierski M, Shi Z, Kalendralis P, Welch M, Nissen HD, Jaffray D, Dekker A, Wee L. Stability of radiomic features of apparent diffusion coefficient (ADC) maps for locally advanced rectal cancer in response to image pre-processing. *Phys Med* 2019; **61**: 44-51 [PMID: 31151578 DOI: 10.1016/j.ejmp.2019.04.009]

43 **Choi MH**, Oh SN, Rha SE, Choi JI, Lee SH, Jang HS, Kim JG, Grimm R, Son Y. Diffusion-weighted imaging: Apparent diffusion coefficient histogram analysis for detecting pathologic complete response to chemoradiotherapy in locally advanced rectal cancer. *J Magn Reson Imaging* 2016; **44**: 212-220 [PMID: 26666560 DOI: 10.1002/jmri.25117]

44 **Wedeen VJ**, Hagmann P, Tseng WY, Reese TG, Weisskoff RM. Mapping complex tissue architecture with diffusion spectrum magnetic resonance imaging. *Magn Reson Med* 2005; **54**: 1377-1386 [PMID: 16247738 DOI: 10.1002/mrm.20642]

45 **De Robertis R**, Maris B, Cardobi N, Tinazzi Martini P, Gobbo S, Capelli P, Ortolani S, Cingarlini S, Paiella S, Landoni L, Butturini G, Regi P, Scarpa A, Tortora G, D'Onofrio M. Can histogram analysis of MR images predict aggressiveness in pancreatic neuroendocrine tumors? *Eur Radiol* 2018; **28**: 2582-2591 [PMID: 29352378 DOI: 10.1007/s00330-017-5236-7]

46 **Dinapoli N**, Barbaro B, Gatta R, Chiloiro G, Casà C, Masciocchi C, Damiani A, Boldrini L, Gambacorta MA, Dezio M, Mattiucci GC, Balducci M, van Soest J, Dekker A, Lambin P, Fiorino C, Sini C, De Cobelli F, Di Muzio N, Gumina C, Passoni P, Manfredi R, Valentini V. Magnetic Resonance, Vendor-independent, Intensity Histogram Analysis Predicting Pathologic Complete Response After Radiochemotherapy of Rectal Cancer. *Int J Radiat Oncol Biol Phys* 2018; **102**: 765-774 [PMID: 29891200 DOI: 10.1016/j.ijrobp.2018.04.065]

47 **Cui Y**, Yang X, Shi Z, Yang Z, Du X, Zhao Z, Cheng X. Radiomics analysis of multiparametric MRI for prediction of pathological complete response to neoadjuvant chemoradiotherapy in locally advanced rectal cancer. *Eur Radiol* 2019; **29**: 1211-1220 [PMID: 30128616 DOI: 10.1007/s00330-018-5683-9]

48 **Chen H**, Shi L, Nguyen KNB, Monjazeb AM, Matsukuma KE, Loehfelm TW, Huang H, Qiu J, Rong Y. MRI Radiomics for Prediction of Tumor Response and Downstaging in Rectal Cancer Patients after Preoperative Chemoradiation. *Adv Radiat Oncol* 2020; **5**: 1286-1295 [PMID: 33305090 DOI: 10.1016/j.adro.2020.04.016]

49 **van Heeswijk MM**, Lambregts DMJ, Maas M, Lahaye MJ, Ayas Z, Slenter JMGM, Beets GL, Bakers FCH, Beets-Tan RGH. Measuring the apparent diffusion coefficient in primary rectal tumors: is there a benefit in performing histogram analyses? *Abdom Radiol (NY)* 2017; **42**: 1627-1636 [PMID: 28160039 DOI: 10.1007/s00261-017-1062-2]

50 **Nie K**, Shi L, Chen Q, Hu X, Jabbour SK, Yue N, Niu T, Sun X. Rectal Cancer: Assessment of Neoadjuvant Chemoradiation Outcome based on Radiomics of Multiparametric MRI. *Clin Cancer Res* 2016; **22**: 5256-5264 [PMID: 27185368 DOI: 10.1158/1078-0432.CCR-15-2997]

Published by **Baishideng Publishing Group Inc**
7041 Koll Center Parkway, Suite 160, Pleasanton, CA 94566, USA
Telephone: +1-925-3991568
E-mail: bpgoffice@wjgnet.com
Help Desk: https://www.f6publishing.com/helpdesk
https://www.wjgnet.com